Macromolecular Research

Article

DOI 10.1007/s13233-020-8127-8

www.springer.com/13233 pISSN 1598-5032 eISSN 2092-7673

Curing Behavior of 4,4'-Diglycidyloxybiphenyl with *p*-Phenylene Diamine Derivatives

Arinola Isa Olamilekan[1]
Hyeonuk Yeo*[,1,2]

[1] Department of Science Education, Kyungpook National University, Daegu 41566, Korea
[2] Department of Chemistry Education, Kyungpook National University, Daegu 41566, Korea

Received March 5, 2020 / Revised May 21, 2020 / Accepted May 31, 2020

Abstract: To expand the applicability of 4,4'-diglycidyloxybiphenyl (BP), the simplest liquid crystalline epoxy derivative, the curing reaction mechanism with *p*-phenylenediamine (*p*-PDA) derivatives under various stereoscopic conditions was investigated through kinetic analyses. Specifically, curing factors such as the starting temperature, heat, and activation energy were studied and analyzed. In particular, the effect of steric hindrance of the hardeners on the mechanism of curing reactions was explored by analyzing isothermal kinetics. It was found that the larger steric hindrance of the curing agents induced the slower curing reaction, and the contribution of the reduction in the self-catalytic curing was more pronounced than the S_N2 reaction. To determine the optimized curing conditions, cured BP materials were fabricated and their glass-transition temperatures and thermal conductivities, which significantly improved over general-purpose epoxy resins owing to the characteristics of the liquid crystal, were investigated.

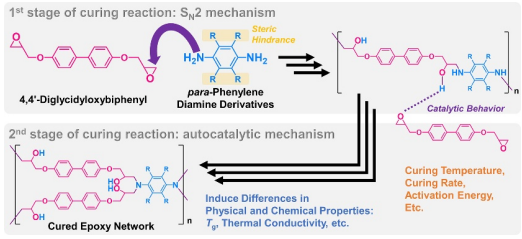

Keywords: epoxy, curing, kinetics, thermosets, thermal conductivity.

1. Introduction

Epoxy resin (ER), a common thermosetting plastic, has excellent resistance to water, chemicals, and weather in addition to strong adhesion, which have made its use possible in many industries.[1-3] The shape of common ER is a highly viscous liquid that is easy to coat and highly permeable with various materials, so it has been widely used in composite materials.[4-7] Due to its outstanding characteristics, new types of ERs continue to be developed, including some special-purpose ERs. Among them, liquid crystal epoxy resin (LCER) has been noted as a promising material.[8-13] Depending on the self-assembly properties of the liquid crystal (LC), LCER is capable of offering excellent mechanical, thermal, and electrical properties.

ERs including LCER are generally polymerized using amines and acid anhydride as a curing agent. The polymerization process mainly involves polyaddition reactions, which forms a cross-linked network, because the majority of ERs and curing agents are multi-functional monomers. This process is called curing or hardening, which induces a large difference in the network structure after polymerization depending on the chemical structure of ERs and curing agents.[14,15] As the formed network structure after curing is the one that determines the major properties of the resultant materials, it is very important to know more about the details of curing agents and curing reaction. As such, many researchers have established methods to predict detailed curing behavior by investigating curing reaction with structural or calorimetric analysis.[16-19] These methods take an empirical method of measuring actual values or changes in structures through experiments and setting for prediction based on them. In particular, in the case of LCER, the majority of its superior characteristics arise from the chemical structures, so the curing-induced network structures are more important than those of normal ERs.[20-22]

Our group has investigated 4,4′-diglycidyloxybiphenyl (**BP**), the LCER with the simplest chemical structure, and reported its interesting properties. In particular, the author was interested in providing information on curing agents and investigating a nature of curing reaction for the diversification of the properties of cured **BP**.[23,24] Providing a library of suitable curing agents for new resins is critical for their practical utilization, and information on typical diamine curing agents has already been reported. As a result, it was reported that depending on the degree of basicity of diamines, the starting temperature of the curing reaction could be predicted. However, previous studies simply discussed only the basicity of diamines without consideration of the stereoscopic effect of substrates during the curing reaction by a bimolecular nucleophilic substitution reaction (S_N2) mechanism. Although it is not possible to investigate the reaction of all materials that can be used as curing agents, the author investigated the curing reaction of **BP** with *para*-phenylenediamine (*p*-PDA) derivatives as a model system, which can help predict the stereoscopic effect of the curing agents. In particular, this establishes curing prediction for a new LCER, which not only enables comparison with a general-purpose epoxy resin system, but also reinforces its own application. In this study, the author used a series of *p*-PDA samples with one to four methyl groups on the benzene ring inducing steric hindrance for curing **BP**. In addition, the curing behavior was investigated using differential scanning calorimetry (DSC), and then the data were interpreted by an autocatalytic curing model

Acknowledgment: This research was supported by Kyungpook National University Research Fund, 2017.

***Corresponding Author:** Hyeonuk Yeo (yeo@knu.ac.kr)

to obtain details of curing reaction. This report will provide systematic information for controlling the properties of the resultant cured **BP** materials.

2. Experimental

2.1. Materials

4,4′-Diglycidyloxybiphenyl (**BP**) with an epoxy equivalent weight (EEW) of about 190 g/eq was prepared as a bifunctional epoxy resin following a previous report.[9] The curing agents, *para*-phenylenediamine (*p*-PDA) derivatives, were obtained from TCI (Japan) and used without further purification. Each curing agent was abbreviated based on its IUPAC name as follows: benzene-1,4-diamine (**BD**), which is the same compound as *para*-phenylenediamine; 2-methylbenzene-1,4-diamine (**MBD**); 2,5-dimethylbenzene-1,4-diamine (**DBD**); and 2,3,5,6-tetramethyl-benzene-1,4-diamine (**TBD**). Other chemicals were purchased from Daejung Chemicals (Korea) and used as received.

2.2. Kinetic analysis

Each stoichiometric mixture of **BP** and curing agents was fabricated by preparing the respective dimethylformamide (DMF) solution and then by removing the solvent in vacuo under 80 °C. Since all of the **BP** and the used curing agent samples were in the solid state at room temperature, the solution mixing method was used to prepare homogeneous mixtures. Then, the details of the curing reaction were investigated by using several measurement modes employing differential scanning calorimetry (DSC, Q2000, TA Instruments, USA). About 10 mg of a specimen was used for each measurement, and dynamic DSC measurements were carried out first for setting isothermal mode measurement conditions. The isothermal curves of various curing systems were then recorded at specific temperature points and the details of curing reaction and kinetics were analyzed by fitting the curves to the original Kamal model, expressed by Eq. (1).[25,26]

$$\dot{\alpha} = \frac{d\alpha}{dt} = k\alpha^m(1-\alpha)^n \quad (1)$$

where $d\alpha/dt$ is the curing reaction rate, α is the degree of conversion, k is the rate constant, m is the reaction order of the autocatalytic reaction, and n is the reaction order of the bimolecular nucleophilic substitution (S_N2) reaction.

2.3. Preparation and analysis of cured epoxy resins

To investigate the thermal properties of cured materials, round-shaped bulk specimens were prepared by following method. First, the stoichiometric mixtures of **BP** and each curing agent were well ground and mixed in the solid state. Then, the fine powders were put into a metal mold (diameter: 20 mm, thickness: adjustable) and cured using a hot press under optimized heating conditions. Glass transition temperatures (T_gs) of the cured epoxy resins were investigated from dynamic DSC curves measured under N_2 gas flow at a heating rate of 20 °C/min. In addition, structural analysis according to curing reaction progress was performed on the **TBD** system through Fourier-transform infrared spectroscopy (FT-IR, FT/IR-4100, Jasco, Japan) for a more detailed analysis of the curing mechanism. FT-IR measurements were carried out using cured **TBD** samples prepared at 120 °C with several curing times. The detailed information can be found in the Supplementary Material. Thermal conductivities of the materials were measured by a thermal conductivity measurement system (TPS 2500S, Hot Disk, Sweden).[27]

3. Results and discussion

3.1. Curing system

p-PDA derivatives used for curing **BP** were as follows: 2-methylbenzene-1,4-diamine (**MBD**), 2,5-dimethylbenzene-1,4-diamine (**DBD**), and 2,3,5,6-tetramethylbenzene-1,4-diamine (**TBD**) in addition to benzene-1,4-diamine (**BD**, the same as *p*-PDA). Several methyl-modified *p*-PDA derivatives were employed as curing agents for the replacement of four aromatic hydrogen positions in **BD**. Although 2,3,5-trimethylbenzene-1,4-diamine was excluded due to its low commercial availability, it was thought that it would have no significant effect on the stereochemical effect investigation of curing agents in the curing reaction, which is the purpose of this study. The chemical structures of all the detailed compounds can be found in Figure 1.

In order to investigate curing reaction starting temperature (T_{onset}), maximum exothermic temperature (T_{peak}), and reaction heat (ΔH_T), dynamic DSC analysis was carried out. First, four kinds of stoichiometric curing mixtures with **BP** and each diamine were prepared by mixing in the DMF solution followed by evaporation of the solvent. Solvent removal was carried out at the lowest temperature possible to avoid occurring curing. Then, DSC curves of each sample were recorded from room temperature to the temperature at which no exothermic reactions were observed. The dynamic DSC curves are depicted in Figure 1 and the details of curing agents and curing reaction are summarized in Table 1. All curing agents had a similar structure, but the curing behavior with **BP** was found to be totally different. Each curing system showed a similar T_{onset} around 120 °C except for the **MBD** system,

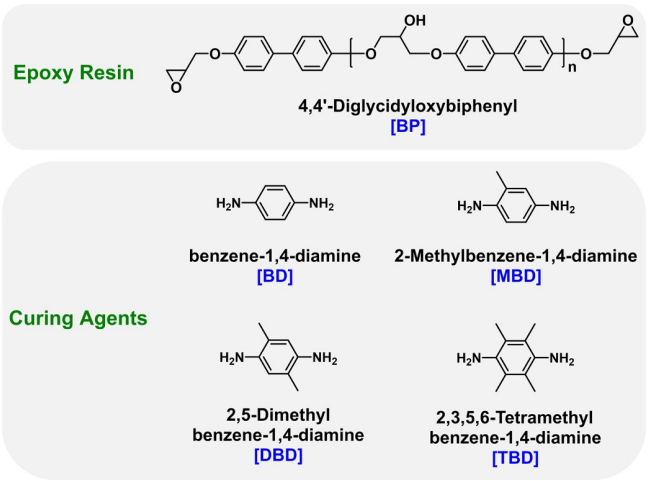

Figure 1. Chemical structures and abbreviations.

Table 1. Curing agents and details of the corresponding curing reaction

Curing agent	T_m[a] (°C)	pK_a	T_{onset}[e] (°C)	T_{peak}[e] (°C)	ΔH_T[e] (J g^{-1})
BD (=*p*-PDA)[f]	138-143	6.20[b]	121.1	135.5	380.0
MBD	64	6.39[c]	111.0	128.4	301.6
DBD	147-151	6.14[d]	124.2	143.0	310.8
TBD	150-155	6.11[d]	122.0	157.0	331.5

[a]Melting temperature obtained from the suppliers. [b]See reference 31. [c]See reference 32. [d]See reference 33. [e]Values from dynamic DSC scans. [f]See reference 24.

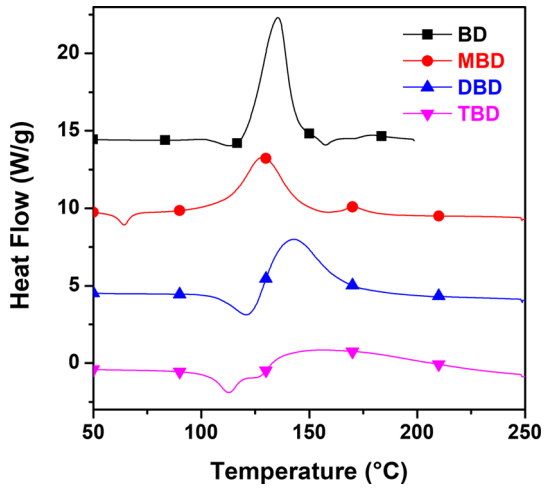

Figure 2. Dynamic DSC curves of various curing systems (heating rate: 20 °C/min; N_2 atmosphere).

which exhibited a slightly lower value of 111 °C. The values of T_{peak} tended to increase in the order **BD**, **DBD**, and **TBD** except **MBD**. Specifically, T_{peak} of **BD** was found at 135.5 °C, **MBD** at 128.4 °C, **DBD** at 143 °C, and **TBD** at 157 °C. In addition, in the case of ΔH_T, it was found that the value of **BD** was rather high. However, the ΔH_T values of the other curing agents were also in the range of curing reaction heat of general ERs.[28-30]

The overall results of the curing reaction could be interpreted as follows. First, the low T_{onset} and T_{peak} of **MBD** seems to be due to the low melting temperature (T_m) of **MBD** compared to that of other curing agents. Before the curing reaction started, only **MBD** melted at around 65 °C and the curing mixture changed to the liquid phase, which would induce a significant impact on the reaction rate. Therefore, **MBD** was considered to have low T_{onset} because it had greater fluidity at the same temperature than other systems in which curing reaction occurred in the solid state. The same is the reason for the low T_{peak} of **MBD**. Secondly, apart from the abovementioned reason for **MBD**, a clear difference was observed in the trends of T_{onset} and T_{peak}. The T_{onset} of **MBD** was slightly lower, but the overall values were almost the same. This was because the curing reaction originated from the nucleophilic attack of a lone pair on the nitrogen atom *via* an S_N2 mechanism,[34,35] and the basicity values for the diamines inferred from pK_a values were nearly identical. On the other hand, the values of T_{peak} showed a clear difference of more than 20 °C for different curing agents. This could be attributed to the stereoscopic effect, another factor that controls the reaction speed of an S_N2 reaction. From the DSC curve of **TBD** with the largest steric hindrance, T_{peak} was 157 °C, but the curing reaction continued over 200 °C, which could be clearly interpreted as a stereochemical factor. In addition, the autocatalytic effects of the hydroxyl group of the intermediate during curing could also be controlled by steric hindrance.[36] In other words, while T_{onset} was associated with the basicity, T_{peak} was dominated by the nucleophilicity of curing agents. Finally, with regard to ΔH_T, it was reasonable that **BD** had the largest ΔH_T. Because the value of ΔH_T meant not the calorific value per unit such as mole but the calorific value per gram, so it should be greatest for **BD**, which has the lowest molecular weight. However, the values of ΔH_T seemed to show no particular tendency. This would be because the endothermic curves derived from the LC transition of **BP** that occurred at around 156 °C in the pure state overlapped with the exothermic curves of the curing reaction. No clear eutectic points were observed, and the curing curves could also be identified as asymmetric.

3.2. Isothermal kinetics studies of curing reaction

From the results of the dynamic DSC measurements, measurement conditions of isotherms for kinetic analysis were determined. Isothermal DSC data were collected at 10 °C intervals between values around T_{onset} and T_{peak} for each system. The detailed conditions of measured temperature were as follows: 110~140 °C for **BD**; 120~150 °C for **MBD**; 120~160 °C for **DBD**; and 110~150 °C for **TBD**. In addition, in the case of **BD**, the data at 110, 120, and 130 °C were based on a previous report[20] and the data at 140 °C were newly added to improve the accuracy of the kinetic analysis. Isotherm measurements were carried out by the following process: the sample pan was injected to the DSC chamber after being heated to the setting temperature, and the isothermal curve was recorded until no more exothermic reaction occurred. Then, the obtained isotherms, which were functions of heat flow (dH/dt) and time (t), were converted into functions of the curing reaction rate ($d\alpha/dt$) and t for analyzing the curing kinetics using Eq. (1) by dividing the values of each ΔH_T.[21,22]

In this regard, the converted curves for $d\alpha/dt$ as a function of t at each temperature are shown in Figure 3. In all systems, an increase in temperature resulted in a dramatic increase in the reaction rate. In addition, it was intuitively confirmed that, at the same temperature, the reaction rate was fast in the order **BD** > **MBD** > **DBD** > **TBD**. To be specific, based on the curves at 130 °C, a temperature above the T_{onset} of all systems, the time at which a decrease in $d\alpha/dt$ signifying the completion of curing was noted was as follows: 1.1 min for **BD**, 1.4 min for **MBD**, 2.2 min for **DBD**, and 6.2 min for **TBD**.

At the maximum peaks of the plots, the values of curing reaction rate and time were calculated and listed in Table 2 as $(d\alpha/dt)_p$ and t_p, respectively. Using the factors, $(d\alpha/dt)_p$ and t_p,

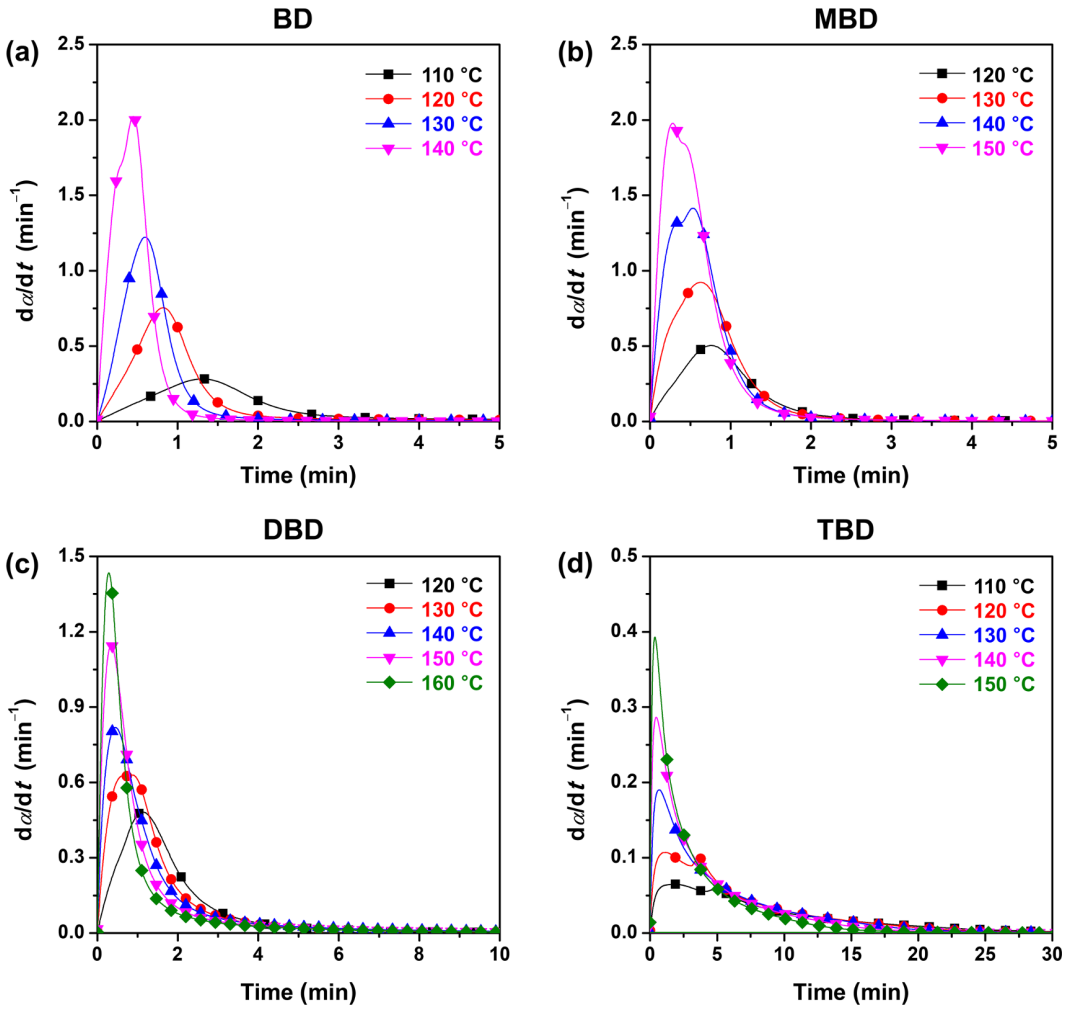

Figure 3. The plots of reaction rate ($d\alpha/dt$) *vs.* time for systems involving (a) **BD**, (b) **MBD**, (c) **DBD**, and (d) **TBD**.

Table 2. Kinetic factors of curing reactions

Curing agents	Curing temperature (°C)	t_p [a]	$(d\alpha/dt)_p$ [a] (min^{-1})	α_p [a]	m [b]	n [b]	k [b] (min^{-1})	E_a [c] (kJ/mol)	A [c] (×10^6 min^{-1})
BD [d]	110	1.30	0.367	0.385	1.450	2.672	3.176	34.369	0.18
	120	0.82	0.754	0.443	1.161	1.880	5.887		
	130	0.60	1.222	0.467	0.997	1.521	6.948		
	140	0.45	2.023	0.543	0.759	1.068	7.123		
MBD	120	0.76	0.505	0.400	0.938	1.752	3.004	38.025	0.35
	130	0.63	0.923	0.430	0.800	1.489	4.321		
	140	0.53	1.415	0.472	0.667	1.322	5.410		
	150	0.28	1.978	0.257	0.588	1.355	6.958		
DBD	120	1.13	0.482	0.350	0.703	1.477	1.885	43.292	0.98
	130	0.87	0.630	0.381	0.568	1.573	2.329		
	140	0.45	0.819	0.223	0.506	1.887	2.886		
	150	0.34	1.146	0.231	0.544	1.962	4.372		
	160	0.28	1.435	0.234	0.611	2.180	6.392		
TBD	110	1.84	0.065	0.138	0.220	1.189	0.119	57.150	7.41
	120	1.16	0.107	0.114	0.222	1.267	0.197		
	130	0.69	0.190	0.102	0.163	1.452	0.286		
	140	0.46	0.286	0.096	0.169	1.586	0.443		
	150	0.36	0.393	0.099	0.198	1.735	0.660		

[a]The values at the maximum of $d\alpha/dt$. [b]The values obtained from the autocatalytic model. [c]The values calculated from Arrhenius plots. [d]The data at 110, 120, and 130 °C were cited from reference 24.

made it easier to mathematically compare the reaction behavior at each condition. First, although there was a slight difference in the values observed for the curing agents, as the temperature rose, for the same curing system, the t_p became smaller and $(d\alpha/dt)_p$ became larger. When the temperature increased by 10 °C, on an average, it was found that t_p decreased by 0.70 times and $(d\alpha/dt)_p$ increased by 1.56 times. This tendency did not involve a large error for every temperature interval. Secondly, for comparison between the curing agents, the values of $(d\alpha/dt)_p$ and t_p at 130 °C were as follows: 1.222 min^{-1} and 0.60 min for **BD**, 0.923 min^{-1} and 0.63 min for **MBD**, 0.630 min^{-1} and 0.87 min for **DBD**, and 0.190 min^{-1} and 0.69 min for **TBD**. Considering $(d\alpha/dt)_p$, which could be regarded as representative of the overall reaction rate, there was a large difference depending on the curing agents, and the curing agents with large steric hindrance caused slow curing. However, interestingly, it was confirmed that there was not much difference between the values of t_p for the curing agents. This was probably because steric hindrance of curing agents had only a minor effect on the S_N2 reaction that occurred in the early stage of the reaction. Conversely, as the molecular weight of the reaction intermediate increased, the stereoscopic effect of the bulky methyl groups might be more pronounced. Even then, if the curing is only dominated by a typical S_N2 mechanism, $(d\alpha/dt)_p$ and t_p must be present early in the reaction. However, in all systems, there was a maximum point along with the progress of the reaction, rather than in the initial stage. This clearly indicated that a catalytic acceleration existed along with a reduction in the reactants. Therefore, it was obvious that all curing reaction had two step mechanism consist of S_N2 reaction followed by self-catalytic stages. In addition, in both curing mechanisms, steric hindrance of curing agents was found to inhibit the reaction and reduce the rate although it did not affect T_{onset} and t_p a lot.

Next, for all systems, the function of $d\alpha/dt$ was integrated over t to calculate the degree of conversion (α) as a function of t. In the process, the maximum value of was set to 1 in the infinity of t. The plots of α are depicted in Figure 4. All reactions were very fast in the early stages of the curing, but when a certain level of α was reached, the reaction speed was significantly reduced. In particular, focusing on the initial stages of the reaction, there was a delay in the rate of increase of α in all systems except the one with **TBD**, which showed the fastest rate of α increase at the beginning of the reaction. In other words, only **TBD** underwent the fastest reaction in the early stages, so it could be seen as the smallest autocatalytic effect.

At 130 °C for each system, the times which the half of reaction proceeded ($t_{\alpha=0.5}$) and at which the reaction was almost complete ($t_{\alpha=0.9}$) were as follows: 0.62 and 1.16 min for **BD**, 0.70 and 1.52 min for **MBD**, 1.12 and 4.50 min for **DBD**, and 3.81

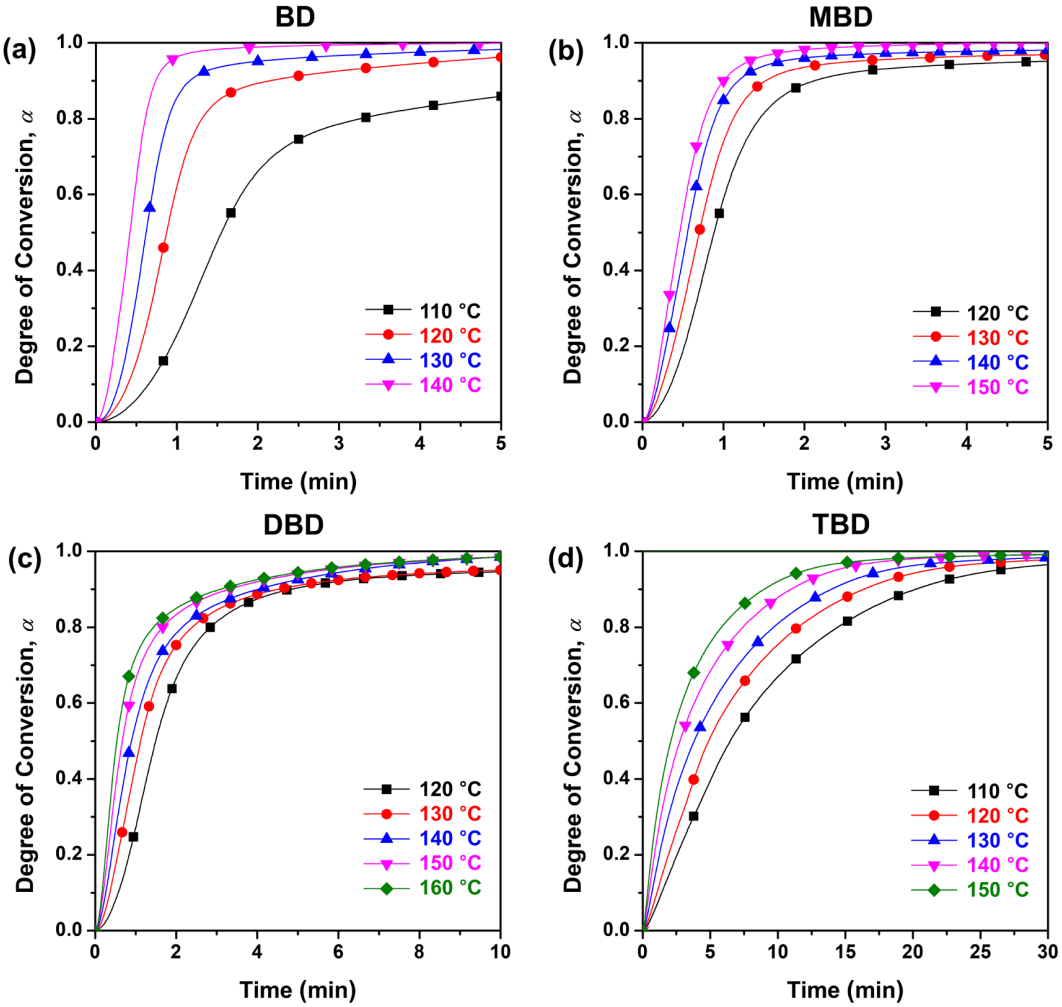

Figure 4. The plots of degree of conversion (α) vs. time for systems involving (a) **BD**, (b) **MBD**, (c) **DBD**, and (d) **TBD**.

and 13.95 min for **TBD**, respectively. At the same temperature, the times to reach the same a were perfectly consistent with the sequence of reaction rates. Since the basicity of the derivatives of *p*-PDA were almost identical, the direct comparison of the reaction times clearly indicated the effect of nucleophilicity of curing agents including the stereoscopic factors. In addition, the average reduction ratios of $t_{\alpha=0.5}$ with temperature increase of 10 °C were as follows: 0.66 for **BD**, 0.80 for **MBD**, 0.77 for **DBD**, and 0.75 for **TBD**. Although the value of **BD** deviated slightly from the trend due to its extremely fast reaction, the values of the rest systems were similar, so utilizing them would be possible to estimate roughly the time required for hardening.

The values of α at the time of maximum $d\alpha/dt$ (named α_p) are listed in Table 2. In the mechanism of curing, a large α_p means that an autocatalytic reaction is dominant, and a small value indicates that an S_N2 reaction is dominant. There were differences in the values depending on the temperature, but typical tendencies were identified. **BD** and **DBD** systems tended to be high in α_p, while the values of **DBD** and **TBD** systems were identified with small. In particular, among them, **TBD** had an absolutely very small values at all temperature. Accordingly, the curing reaction of **BD** and **DBD** were predominantly autocatalytic and the reaction of the rest were dominated by S_N2 reaction. In addition, when comparing the α_p values between the temperatures for each curing agent, with the exception of **BD**, the values of α_p appeared small at high temperatures. Thus, S_N2 curing prevailed at high temperatures and self-catalytic curing was dominant at low temperatures. This result was in line with the previously reported tendency for the typical diamine curing agents.[20] In the case of **BD**, meanwhile, it showed the opposite tendency, which indicated that autocatalytic mechanism predominated at high temperatures. In the end, autocatalytic reaction was found to be more affected by stereoscopic hindrance than S_N2. Therefore, **DBD** and **TBD** were relatively inferior in autocatalysis and appeared to be fairly dominant on S_N2. This did not mean that S_N2 is more likely to occur than other hardener, and because of its slower overall reaction process, simply S_N2 was more dominant in proportion.

The values of $d\alpha/dt$ were plotted as a function of α to obtain all kinetic factors through the interpretation of the Eq. (1).[21,22] The plots are shown in Figure 5 and the rest of kinetic parameters such as the rate constant (k) and reaction orders (m and n) determined by fitting with Eq. (1) are listed in Table 2. The obtained parameters at 130 °C for each system were as follows: 6.948 min^{-1}, 0.997, and 1.521 for **BD**; 4.321 min^{-1}, 0.800, and 1.489 for **MBD**; 2.329 min^{-1}, 0.568, and 1.573 for **DBD**; and 0.286 min^{-1}, 0.163, and 1.452 at 140 °C for **TBD**. The listed order was k, m, and n. Using the values clearly made it possible to compare reaction kinetics and mechanism in various conditions for several curing agents. First, from the propensity of the k values

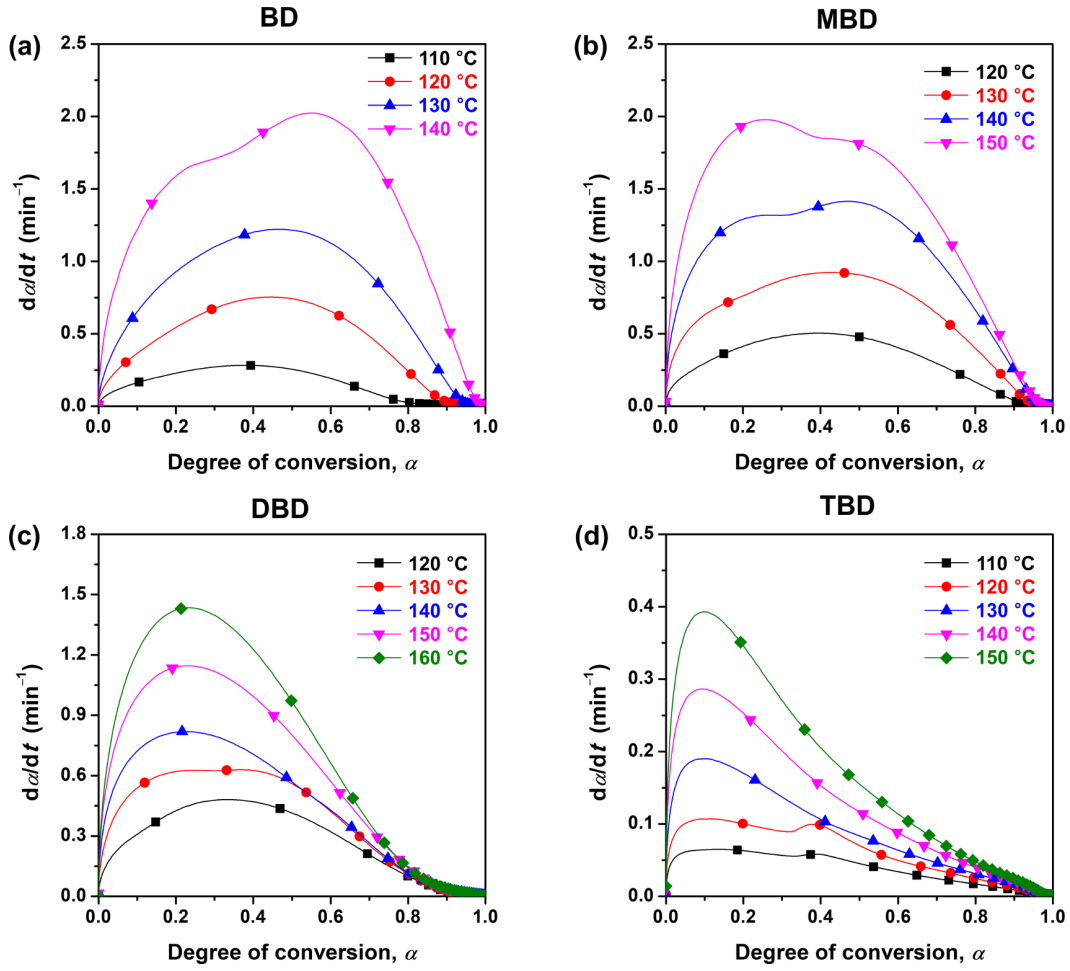

Figure 5. The plots of reaction rate ($d\alpha/dt$) *vs.* degree of conversion (α) for systems involving (a) **BD**, (b) **MBD**, (c) **DBD**, and (d) **TBD**.

at the same temperature, it was clear that the reaction rates were **BD**, **MBD**, **DBD**, and **TBD** in the order of fast reaction listed first. In addition, the values of *n*, which meant n^{th} order reaction by S_N2, were almost identical, and the values of *m*, which indicated the reaction order of autocatalytic reaction, were found to vary significantly. Eventually, the values of reaction order of S_N2 did not change significantly depending on the curing agent, but it was clear that the reaction order of the autocatalysis was significantly different from the steric condition of the curing agents. In addition, from the values of reaction order for each curing agent, as the temperature increased, it was confirmed that both values decreased in **BD** and **MBD**. But, in **DBD** and **TBD**, the values of *m* were only slightly varied, and the values of *n* tended to increase. From these results, it was once again confirmed that the contribution of S_N2 mechanism in **DBD** and **TBD** increased with increasing temperature.

3.3. Arrhenius behavior of curing reaction

Based on the *k* values measured at various temperatures, the Arrhenius plots were depicted to obtain the values of activation energy (E_a) and pre-exponential factor (A) in the curing systems, as shown in Figure 6. Each E_a and A was obtained from the slope of the Arrhenius plot and the *Y* intercept, and the values are listed in Table 2. The calculated values of E_a and A as follows: 34.369 kJ mol^{-1} and 1.8 α 10^5 min^{-1} for **BD**, 38.025 kJ mol^{-1} and 3.5 × 10^5 min^{-1} for **MBD**, 43.292 kJ mol^{-1} and 9.8 × 10^5 min^{-1} for **DBD**, and 57.150 kJ mol^{-1} and 7.41 × 10^6 min^{-1} for **TBD**. The result obviously suggested that the faster the reaction curing system is, the smaller is the E_a value. In addition, except for **TBD**, it was confirmed that a somewhat lower E_a values than common epoxy curing systems, which would induce the overall curing reaction to be very fast.[37,38] This was consistent with the almost complete curing observed within five minutes. In general, the reaction with small E_a starts to occur at low temperature. However, in this study, this tendency was not observed, which was thought to be because the curing reaction was occurred in multiple stages and the compared systems had their own curing characteristics. In addition, the Arrhenius plots of the kinetic factors, $(d\alpha/dt)_p$ and t_p are depicted in Figure S3 and S4. Utilizing information from these factors with Arrhenius behavior, it would be greatly helpful to investigate the curing behavior under specific temperature conditions.

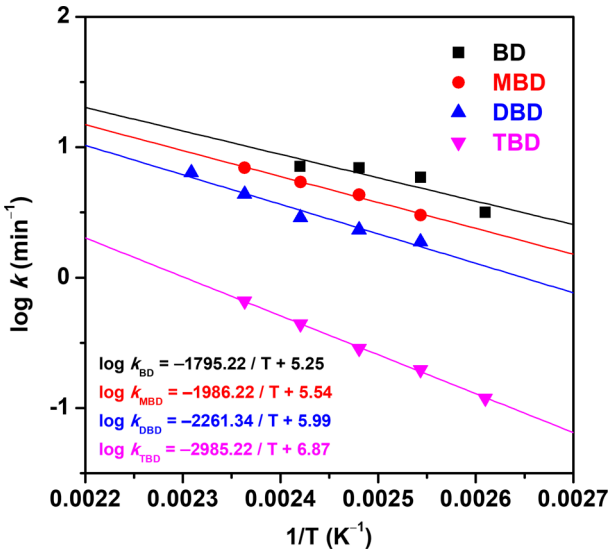

Figure 6. Arrhenius plots of the rate constant (*k*).

Table 3. Thermal properties of cured materials

Curing agents	T_g[a] (°C)	Thermal conductivity[b] (W/m·K)
BD	145.1[c]	0.36
MBD	200.0	0.32
DBD	161.1	0.38
TBD	185.5	0.37

[a]Glass transition temperature from DSC measurements (heating rate: 20 °C/min; N_2 atmosphere). [b]Measured by Hot Disk according to ISO 22007-02. [c]See reference 24.

3.4. Thermal properties of cured BP

Cured epoxy materials were manufactured under the optimized condition by hot-press molding according to the information obtained from curing kinetic analysis. The curing temperature was set above the eutectic point to take advantage of the LC behavior of **BP**. The resulting cured epoxy specimens exhibited the color of pale yellow. Then, basic properties such as glass transition temperature (T_g) including thermal conductivity, which could utilize the best use of the LC nature, were investigated. The measured values were listed in Table 3 and the curves depicted in Figure S5. The values of T_g ranged from 145 to 200 °C and was found to be significantly higher than the general-purpose ERs.[39] In particular, the epoxy cured by **DBD** showed a very high T_g of 200 °C. In fact, it was expected that there would be a tendency of T_g depending on the three-dimensional structure of the curing agents, but no particular propensity was confirmed. Perhaps because **DBD** formed the most asymmetrical cured molecular structure, this was considered to have resulted in a high T_g. In addition, thermal conductivity was measured with a Hot Disk instrument, and the values were 0.36, 0.32, 0.38, and 0.37 W/m×K in the order **BD**, **MBD**, **DBD**, and **TBD**, respectively. There was no particular trend, but all values were very high compared to those of general-purpose ERs.[40] Considering that **BP** cured with popular curing agents had a thermal conductivity of about 0.3 W/mK,[9] it was confirmed that *p*-PDA derivatives could grant a considerably high thermal conductivity. Compared to conventional curing system, these curing systems contained small amounts of hardeners in mass proportion due to the small molecular weight of the curing agents, which would affect significantly the results inducing the highly ordered LC alignment. Furthermore, the reason for the high thermal conductivity might be that the structure with high aromatic ratio was maintained to help the LC array.

4. Conclusion

In this work, a thorough investigation was conducted into the reaction mechanism and kinetics of several curing systems using *p*-PDA derivatives that differed in the number of methyl groups as substituents, as a potential curing agent for **BP**, the

simplest LCER. Although there was no difference in the basicity of diamines according to the presence of the substituents, it was confirmed that there was a large difference in the rate of the curing reaction depending on the stereochemical factors, which caused varied curing times. In addition, based on the results of isothermal DSC studies, the curing reaction was interpreted by the autocatalytic model, which confirmed that the contribution of the two representative curing mechanisms was significantly different for the curing agents. The rate of the curing reaction decreased in the order **BD**, **MBD**, **DBD**, and **TBD**, in the same order as the order in which the steric hindrance of the hardeners increased. This could also be confirmed from the calculation results of the activation energy, and it was clear that an increase in stereoscopic disturbances would bring about a large activation energy. In addition, in terms of the reaction mechanism, it was found that the more steric hindrance in the curing agents induced the domination of S_N2 mechanism and S_N2 reaction more contributed to curing reaction than autocatalytic behavior at higher temperatures. Lastly, the cured epoxy materials were fabricated under the obtained optimal conditions and their T_g and thermal conductivity values were investigated. The specific tendency of the particular properties to be associated with steric hindrance could not be identified, but all of the cured BP had higher T_g and thermal conductivity relative to the general general-purpose ERs. In this regard, the results of this study will not only provide important information on reaction kinetics for selecting the hardener, but will also provide a wide range of knowledge leading up to the prediction of the properties.

Supporting information: Information is available regarding structure analysis by FT-IR spectroscopy during curing reaction, Arrhenius behaviors of $(da/dt)_p$ and t_p, and DSC curves of cured materials. The materials are available *via* the Internet at http://www.springer.com/13233.

References

(1) C. May, *Epoxy Resins: Chemistry And Technology*, CRC Press, New York, 1988.
(2) S. Wang, S. Q. Ma, C. X. Xu, Y. Liu, J. Y. Dai, Z. B. Wang, X. Q. Liu, J. Chen, X. B. Shen, J. J. Wei, and J. Zhu, *Macromolecules*, **50**, 1892 (2017).
(3) Y. O. Kim, J. Cho, H. Yeo, B. W. Lee, B. J. Moon, Y. M. Ha, Y. R. Jo, and Y. C. Jung, *ACS Sustain. Chem. Eng.*, **7**, 3858 (2019).
(4) C. F. Wang, M. Zhao, J. Li, J. L. Yu, S. F. Sun, S. S. Ge, X. K. Guo, F. Xie, B. Jiang, E. K. Wujcik, Y. D. Huang, N. Wang, and Z. H. Guo, *Polymer*, **131**, 263 (2017).
(5) J. Chen, X. Y. Huang, Y. K. Zhu, and P. K. Jiang, *Adv. Funct. Mater.*, **27**, 1604754 (2017).
(6) X. H. Cao, X. D. Wei, G. J. Li, C. Hu, K. Dai, J. Guo, G. Q. Zheng, C. T. Liu, C. Y. Shen, and Z. H. Guo, *Polymer*, **112**, 1 (2017).
(7) J. Han, G. Du, W. Gao, and H. Bai, *Adv. Funct. Mater.*, **29**, 1900412 (2019).
(8) W. B. Shen, L. Wang, G. Chen, C. X. Li, L. Y. Zhang, Z. Yang, and H. Yang, *Polymer*, **167**, 67 (2019).
(9) H. Yeo, A. M. Islam, N. H. You, S. Ahn, M. Goh, J. R. Hahn, and S. G. Jang, *Compos. Sci. Technol.*, **141**, 99 (2017).
(10) Y. Kim, H. Yeo, N. H. You, S. G. Jang, S. Ahn, K. U. Jeong, S. H. Lee, and M. Goh, *Polym. Chem.*, **8**, 2806 (2017).
(11) J. M. McCracken, V. P. Tondiglia, A. D. Auguste, N. P. Godman, B. R. Donovan, B. N. Bagnall, H. E. Fowler, C. M. Baxter, V. Matavulj, and J. D. Berrigan, *Adv. Funct. Mater.*, **29**, 1903761 (2019).
(12) S. Tanaka, F. Hojo, Y. Takezawa, K. Kanie, and A. Muramatsu, *ACS Omega*, **3**, 3562 (2018).
(13) A. Belmonte, G. C. Lama, G. Gentile, X. Fernandez-Francos, S. De la Flor, P. Cerruti, and V. Ambrogi, *J. Phys. Chem. C*, **121**, 22403 (2017).
(14) A. M. Islam, H. Lim, N. H. You, S. Ahn, M. Goh, J. R. Hahn, H. Yeo, and S. G. Jang, *ACS Macro Lett.*, **7**, 1180 (2018).
(15) W. B. Shen, L. Wang, Y. P. Cao, L. Y. Zhang, Z. Yang, X. T. Yuan, H. Yang, T. M. Jiang, and H. G. Chen, *Polymer*, **172**, 231 (2019).
(16) R. E. Smith, F. N. Larsen, and C. L. Long, *J. Appl. Polym. Sci.*, **29**, 3713 (1984).
(17) E. Mertzel and J. L. Koenig, in *Epoxy Resins and Composites II, Advances in Polymer Science,* K. Dušek, Ed., Springer, Berlin, Heidelberg, 1986, Vol. 75, pp 73-112.
(18) N. Sbirrazzuoli and S. Vyazovkin, *Thermochim. Acta*, **388**, 289 (2002).
(19) R. Hardis, J. L. Jessop, F. E. Peters, and M.R. Kessler, *Compos. Part A: Appl. Sci. Manuf.*, **49**, 100 (2013).
(20) Y. Q. Rao, A. D. Liu, and K. O'Connell, *Polymer*, **142**, 109 (2018).
(21) Y. Z. Li, Y. Zhang, O. Rios, J. K. Keum, and M. R. Kessler, *Soft Matter*, **13**, 5021 (2017).
(22) X. Yang, J. Zhu, D. Yang, J. Zhang, Y. Guo, X. Zhong, J. Kong, and J. Gu, *Compos. Part B: Eng.*, **185**, 107784 (2020).
(23) H. Yeo, *Polymer*, **159**, 6 (2018).
(24) H. Yeo, *Polymer*, **168**, 209 (2019).
(25) M. Keenan, *J. Appl. Polym. Sci.*, **33**, 1725, (1987).
(26) M. Kamal and S. Sourour, *Polym. Eng. Sci.*, **13**, 59 (1973).
(27) S. E. Gustafsson, *Rev. Sci. Instrum.*, **62**, 797 (1991).
(28) C. Riccardi, H. Adabbo, and R. Williams, *J. Appl. Polym. Sci.*, **29**, 2481 (1984).
(29) K. Horie, H. Hiura, M. Sawada, I. Mita, and H. Kambe, *J. Polym. Sci. Part A-1: Polym. Chem.*, **8**, 1357 (1970).
(30) H. Y. Cai, P. Li, G. Sui, Y. H. Yu, G. Li, X. P. Yang, and S. Ryu, *Thermochim. Acta*, **473**, 101 (2008).
(31) D. D. Perrin, *Dissociation Constants of Organic Bases in Aqueous Solution,* Franklin Book Co., Butterworths, 1972.
(32) A. Meyer and K. Fischer, *Environ. Sci. Eur.*, **27**, 11 (2015).
(33) ACD/Labs, Version 11.02, Advanced Chemistry Development, Inc., Toronto, ON, Canada, www.acdlabs.com, 2020.
(34) D. Rosu, A. Mititelu, and C. N. Cascaval, *Polym. Test.*, **23**, 209 (2004).
(35) S. Vyazovkin and N. Sbirrazzuoli, *Macromolecules*, **29**, 1867 (1996).
(36) V. Špaček, J. Pouchlý, and J. Biroš, *Eur. Polym. J.*, **23**, 377 (1987).
(37) C. Riccardi, H. Adabbo, and R. Williams, *J. Appl. Polym. Sci.*, **29**, 2481 (1984).
(38) R. Thomas, S. Durix, C. Sinturel, T. Omonov, S. Goossens, G. Groeninckx, P. Moldenaers, and S. Thomas, *Polymer*, **48**, 1695 (2007).
(39) J. M. Zhou and J. P. Lucas, *Polymer*, **40**, 5513 (1999).
(40) H. Oh, Y. Kim, and J. Kim, *Polymer*, **183**, 121834 (2019).

